

Vibrational properties of a sodium tetrasilicate glass: *Ab initio* versus Classical Force Fields

Simona Ispas^{*1}, N. Zотов², S. De Wispelaere¹ and W. Kob¹

¹ Laboratoire des Verres, Université Montpellier 2,

Place E. Bataillon, 34095 Montpellier Cedex 5, France

² Mineralogisch-Petrologisches Institut,

University Bonn, Poppelsdorfer Schloss,

D-53115 Bonn, Germany,

(February 7, 2020)

Abstract

We compare some vibrational properties of a sodium tetrasilicate ($\text{Na}_2\text{Si}_4\text{O}_9$) glass model generated by molecular dynamics simulations. The vibrational study has been carried out using a classical valence force fields approach as well as an *ab initio* approach in the framework of the density functional theory. The total and partial vibrational densities of states (VDOS) are presented, and some characteristics of the vibrational modes (participation ratios, correlation lengths) are determined using both approaches. We find that the shapes of the two calculated VDOS as well as those of their corresponding partial VDOS are quite similar, especially for a low-frequency band below 550 cm^{-1} . For the intermediate- and high-frequency ranges, we observe larger discrepancies between the two calculations. Polarized Raman spectra are also calculated from the *ab initio* and the valence-force-field eigenvectors in the bond-polarizability approximation. We find an overall agreement between the calculated parallel (VV) polarized Raman spectra and the corresponding experimental spectrum. Concerning the perpendicular (VH) depolarized Raman spectrum, the comparison of the calculated spectra to the experimental data indicates a need for an additional adjustment of the corresponding bond-polarizability parameters.

PACS numbers: 61.43.Bn, 61.43.Fs, 71.15.Pd, 71.23.Cq

Typeset using REVTeX

^{*}Author to whom correspondence should be addressed: simona.ispas@ldv.univ-montp2.fr

1. INTRODUCTION

The nature of the vibrational excitations of silicate glasses and melts represents a challenging problem of condensed matter physics, glass and earth sciences. Significant experimental and theoretical efforts have been made in order to understand the vibrational properties of these materials, because they provide valuable information about the underlying microscopic structure and other anomalous physical properties of silicate glasses [1]. However, the lack of long-range translational order considerably complicates this task and requires new approaches for measurement, analysis and simulations of the vibrational spectra of glasses and melts as well as a careful investigation on how the vibrational spectra depend on the details of the considered glass (chemical composition, thermal history etc.).

Therefore we compare in the present paper the vibrational density of states (VDOS) and several vibrational characteristics of an *ab initio* model of sodium tetrasilicate glass $\text{Na}_2\text{Si}_4\text{O}_9$ (denoted hereafter NS4) calculated by two different methods. The first calculation is based on an *ab initio* treatment of the interatomic forces and is performed in the framework of the density functional theory, while the second one is performed in the approximation of a classical valence force-field potential which is especially suited for describing the dynamics of partially covalent materials like silicate glasses.

The structure of the NS4 glass has been intensively investigated by different experimental methods [2], reverse Monte Carlo (RMC) [3] as well as classical molecular dynamics (MD) simulations [4,5]. Recently, the structural and electronic properties of the NS4 glass have been modeled by a combined Car-Parrinello and classical MD simulation [6,7]. The attention given to this system is justified by the fact that it can be used as a prototype for more complicated aluminosilicate and hydrous silicate glasses.

The aims of the present study are: (i) to test the quality of the *ab initio* NS4 vibrational dynamics by comparing the calculated and experimental polarized Raman spectra; (ii) to test the quality and the transferability of a previously proposed [5] valence force-field potential for sodium silicate glasses by comparison with *ab initio* calculations; (iii) to analyse the effects of adding Na_2O into a- SiO_2 on the character of the vibrational characteristics of the glass.

2. CALCULATION PROCEDURES

A. The glass model

The amorphous NS4 model used in this study contains 90 atoms (24 silicon atoms, 54 oxygen atoms and 12 sodium atoms) confined in a cubic box of edge length 10.81 Å corresponding to the experimental NS4 mass density of 2.38 g/cm³ [8]. The glass model has been generated using combined classical and *ab initio* molecular dynamics (MD) simulations. We have firstly performed the liquid equilibration, the quench, and the initial part of the low temperature relaxation within the framework of the classical MD, and subsequently we have refined the obtained structure within the framework of the *ab initio* MD. We note that this approach was successfully employed for the study of the structural, electronic and vibrational properties of vitreous SiO_2 [9,10], as well as for a structural and electronic study of vitreous NS4 [6,7].

The classical MD simulations were performed with an interatomic potential which is a modification of the van Beest potential [11] derived in order to study sodium silicates [12]. The NS4 model was generated by quenching a well equilibrated liquid at 3500 K to 300 K, with a quench rate equal to $5 \cdot 10^{13}$ K/s. The glass model obtained this way was relaxed for 70 ps at 300 K. The final atomic coordinates and velocities after the classical relaxation, were used as initial coordinates and velocities for a short (≈ 0.5 ps) *ab initio* MD simulation. The *ab initio* simulations were performed in the framework of the Car-Parrinello (CP) method [13,14] using the CPMD software [15]. The technical details of these simulations were identical to the ones detailed described in Ref. [6], except for the pseudopotential type used for the sodium atoms. During the present CP calculations, we used for the sodium atoms a semi-core Trouiller-Martins norm-conserving pseudopotential [16] instead of the Goedecker semi-core type used previously [6]. This change allowed a better estimation of the internal pressure of the model. Nevertheless, the same structural modifications as reported in [6] occurred immediately after the CP dynamics was switched on. The main structural characteristics (ring distribution, Q-species distribution, etc.) are determined in the classical MD stage. The CP run leads to structural relaxation without significant changes in the network topology.

B. VDOS and Raman spectra calculations

At the end of the CP simulation, the glass model was relaxed to 0 K, and the dynamical matrix was computed numerically by evaluating the second derivatives of the total energy with respect to atomic displacements, which were calculated using the finite differences of the atomic forces. The direct diagonalization of the dynamical matrix provides the eigenvalues $\{\omega_p^{\text{CP}}\}$ and the corresponding normalized eigenvectors $\{\mathbf{e}^{\text{CP}}(\omega_p^{\text{CP}})\}$, $p = 1, \dots, 3N$, where $N = 90$ is the number of atoms in the model. Each eigenvector is a $3N$ -dimensional vector which components are proportional to the displacements of the atoms in mode p .

The *ab initio* NS4 model was then relaxed with a harmonic valence force field (VFF) potential of the Kirkwood-type (for further details, see Ref. [5]). In the present work we used the following values for the stretching force constants α_{ij} : $\alpha_{\text{Si-BO}} = 465 \text{ N/m}$, $\alpha_{\text{Si-NBO}} = 655 \text{ N/m}$, $\alpha_{\text{Na-BO}} = 25 \text{ N/m}$, $\alpha_{\text{Na-NBO}} = 30 \text{ N/m}$, while the bending force constants β_{ijk} were $\beta_{\text{BO-Si-BO}} = \beta_{\text{BO-Si-NBO}} = \beta_{\text{NBO-Si-NBO}} = 35 \text{ N/m}$ and $\beta_{\text{Si-BO-Si}} = 14 \text{ N/m}$, where ‘BO’ denotes the bridging oxygens, while ‘NBO’ denotes the non-bridging oxygens. Within the VFF approach, the dynamical matrix was calculated analytically and was diagonalized using the Householder method. The detailed expressions of the dynamical matrix elements are given elsewhere [17]. The obtained vibrational frequencies will be denoted $\{\omega_p^{\text{VFF}}\}$ and the corresponding eigenvectors $\{\mathbf{e}^{\text{VFF}}(\omega_p^{\text{VFF}})\}$, $p = 1, \dots, 3N$.

The knowledge of all the eigenmodes allows us to calculate the reduced polarized Raman spectra of the NS4 glass model using the bond polarizability approximation (BPA) [18]. As bond polarizability parameters we used the same as the ones of Ref. [5]. Recently, comparison of the Raman scattering mechanism in α -quartz using both *ab initio* methods and the BPA has shown that the BPA reproduces the *ab initio* Raman intensities within 15% [19]. This gives strong support for the application of the BPA for the calculation of the Raman spectra of large models of silicate glasses. The comparison of the Raman spectra calculated independently from the CP and the VFF eigenmodes will allow to investigate

separately the effects of the BPA parameters and the eigenmodes on the accuracy of the Raman spectra calculations.

3. RESULTS

In Fig. 1 we compare the CP and VFF vibrational densities of states. Both VDOS are normalized to one, and we have used the same uniform Gaussian broadening of full width at half maximum $2\sigma = 36 \text{ cm}^{-1}$. In both spectra, we distinguish three ranges: a low-frequency range ($0\text{--}500 \text{ cm}^{-1}$), an intermediate frequency range ($500\text{--}900 \text{ cm}^{-1}$), and a high-frequency range ($900\text{--}1200 \text{ cm}^{-1}$). The low-frequency bands arise generally from Na-O, Si-O bending and rocking motions, the mid-frequency bands arise from complex motion of the Si atoms against the BO atoms while the high-frequency bands arise mainly from Si-BO and Si-NBO stretching motions [5].

In spite of the fact that the intensities of the CP low-frequency bands are slightly higher compared to the VFF ones, both approaches yield almost identical band positions and shapes. Larger discrepancies between the two VDOS are found in the mid- and the high-frequency ranges. The VFF mid-frequency bands are shifted to higher frequencies compared to the CP bands, but the two approaches yield practically the same intensities (same number of vibrational modes). In the high-frequency range the shape of the vibrational bands is generally the same but the VFF bands are shifted to higher frequencies and have larger intensities.

Unfortunately, to the best of our knowledge, there are no VDOS data for the NS4 glass measured by inelastic neutron scattering to compare with our calculations. Therefore we compare in Fig. 2, the calculated and experimentally reduced polarized (VV and VH) Raman spectra. We recall that the so-called reduced spectrum is obtained by multiplying the experimental measured spectrum with the correction factor $\omega/n(\omega) \cdot (\omega - \omega_0)^4$ in order to have a temperature independent quantity ($n(\omega)$ is the Bose factor). The polarized Raman spectra were measured on doubly-polished glass plates in backscattering geometry using the 514.5 nm line of an Ar⁺ laser and a XY triple spectrometer equipped with a liquid-nitrogen cooled CCD detector and confocal entrance optics with 300 s accumulation time per spectral window. In both calculations, the final spectra have been obtained by applying an uniform Gaussian broadening with full width at half maximum equal to 30 cm^{-1} to the calculated Raman intensities. The VV spectra (Fig. 2a) were normalized so that the high-frequency peaks (at about 1100 cm^{-1}) have the same maximum intensity, while the VH spectra (Fig. 2b), were normalized so that the peaks at $\approx 800 \text{ cm}^{-1}$ have similar intensities.

In the VV Raman spectra (Fig. 2a), we distinguish also three bands. The previous calculation [5] of the VV Raman spectra on NS4 glass models have assigned the low-frequency band at about 520 cm^{-1} to symmetric bending of the Si-BO-Si linkages, the mid-frequency band at about 780 cm^{-1} to the Si motions against the BO atoms and the high-frequency band at about 1100 cm^{-1} with a shoulder at about 920 cm^{-1} to the Si-NBO stretching motions.

For the position and the relative intensity of the low-frequency band, a good overall agreement between the experimental and the CP calculated curve is observed although, e.g., the width of the CP band is smaller and the shoulder in the experimental data at about 600 cm^{-1} is not reproduced. The agreement between the low-frequency VFF band and the experimental spectrum is less good - the calculated VFF intensity is stronger and

the maximum peak position is shifted to slightly higher frequencies. In other words, the VFF potential overestimates the amplitudes of the Si-BO-Si symmetric bending vibrations.

The intensity of the CP calculated mid-frequency band is in good agreement with the experiment but its position is shifted approximately 80 cm^{-1} to lower frequencies. The shape of the VFF corresponding band is similar to the experimental one, but we note a smaller intensity and a slight shift to lower frequencies. (see the inset in Fig. 2a).

Concerning the high-frequency band, the position of the main peak is shifted approximately 20 cm^{-1} downwards in the CP case and approximately 20 cm^{-1} upward in the VFF case indicating slightly weaker and slightly stronger Si-NBO interactions, respectively. Both approaches yield much stronger intensity for the 920 cm^{-1} band which arises mainly from Si-NBO stretching vibrations in SiO_4 tetrahedra with 2 NBO per Si (Q^2 species) [5].

The calculated low-frequency bands in the depolarized (VH) spectrum seem to be correctly positioned and to have the same relative intensities (see Fig. 2b, where we have plotted the truncated VH spectra in order to see the details of the spectra in the low- and mid-frequency ranges). In the mid-frequency range, the CP band is broadened and shifted to slightly lower frequencies, while the VFF band is shifted to slightly higher frequencies. In a previous calculation of the VH Raman spectra using a NS4 model generated by RMC simulations [5], the agreement was better in this frequency range. Since the mid-frequency band arises mainly from Si vibrations in Q^4 -species [5], the differences between the present VFF calculation and the results presented in Ref. [5] are to be attributed to the different degree of polymerization of the corresponding models [5,6].

In the high-frequency range (see the inset in Fig. 2b) the calculated depolarized Raman intensities are much weaker in *both* calculated spectra which indicates that the corresponding Si-O bending BPA parameters are too small.

4. DISCUSSION

In order to understand the differences in the VDOS and Raman spectra computed within the CP and VFF approaches, we have analysed first the corresponding partial VDOS. The partial VDOS curves $g_\alpha(\omega)$ in Fig. 3 ($\alpha = \text{Si, BO, NBO, Na}$) have been defined as :

$$g_\alpha(\omega_p) = g(\omega_p) \sum_{i \in \alpha} |\mathbf{e}_i(\omega_p)|^2$$

where $\mathbf{e}_i(\omega_p)$, $i = 1, \dots, N$, are 3-component real space vectors proportional to the displacement of the atom i in mode p .

For the low-frequency bands, we have an overall agreement between the CP and VFF partial VDOS. especially for the Si atoms (Fig. 3a), the NBO atoms (Fig. 3c) and the Na atoms (Fig. 3d). In this frequency range the NBO atoms participate mainly in O-Si-O bending vibrations [5]. The biggest differences are observed in the BO partial VDOS (Fig. 3b), which can explain the differences in the total VDOS in this frequency range.

As can be seen in Fig. 3d, both the CP and VFF calculations predict a dominant Na contribution only in the low-frequency range, but the VFF peak is shifted to slightly ($\approx 28\text{ cm}^{-1}$) lower values. From a previous VFF analysis [5] of the vibrational characteristics of two NS4 structural models obtained by classical MD and RMC simulations, it followed that the Na motion dominated below $\approx 100\text{ cm}^{-1}$. In the present VFF calculation, the Na

contribution reaches a maximum at $\approx 170 \text{ cm}^{-1}$. This shift of the Na low-band to higher frequencies is due to an increase of the Na-O stretching force constants with respect to the values used in Ref. [5] which has led to a much better agreement between the calculated and experimental heat capacities of sodium silicate glasses [20]. .

At intermediate frequencies, the CP and the VFF partial VDOS for the Si, BO and NBO atoms have qualitatively the same shape but the ones for Si and BO partial VDOS are shifted to lower frequencies in the CP calculation (Fig. 3a and b). These shifts are similar to the observed shift of the mid-frequency band in the VV calculated using the CP eigenmodes. So it seems that the CP approach does not describe properly the vibrational dynamics of the Si and BO atoms in the mid-frequency range. Interestingly, the Si motions are enhanced in the CP calculation while the BO motions are enhanced in the VFF calculation.

In contrast to this, the partial VDOS show that in the high-frequency range all of the VFF partial VDOS are enhanced compared to the CP ones. It is natural to expect that this effect is related to the degree of localization of the vibrational modes in the two calculations, because the VFF potential does not have long-range interactions incorporated.

As a measure of the localization of the modes we consider first the participation ratio p_c . The participation ratio for the eigenmode p_c has the following definition [21] :

$$p_c(\omega_p) = \frac{(\sum_{i=1}^N |\mathbf{e}_i(\omega_p)|^2)^2}{N \sum_{i=1}^N |\mathbf{e}_i(\omega_p)|^4}$$

The frequency dependences of the CP and VFF participation ratios are shown in Fig. 4a and 4c. As can be seen from Fig. 4a and 4c, the CP modes are generally more localized than the VFF ones, especially around 200 and above 900 cm^{-1} . This is a new and interesting result because from the form of the VFF potential one would expect just the opposite - the VFF modes to be more localized. The localization is also enhanced near the edges of the three main VDOS bands for both the CP and the VFF participation ratios. These are the so-called band tails containing localized modes, which have been already observed for a larger NS4 glass models in Ref. [5], as well as for silica glass models [5,10,22]. In the CP case, these tails are more pronounced, in particular at the top of the lower band and on both sides of the high-frequency bands. The analysis of the frequency dependences of the vibrational correlation lengths $L_c(\omega_p)$ which are plotted in Fig. 4b and 4d, confirms the localization of the high-frequency modes. The vibrational correlation length is defined (Ref. [23]) as:

$$L_c(\omega_p) = \sqrt{\frac{\sum_{i=1}^N |\mathbf{r}_i - \mathbf{r}_p|^2 |\mathbf{u}_i(\omega_p)|^2}{\sum_{i=1}^N |\mathbf{u}_i(\omega_p)|^2}}$$

where \mathbf{r}_i is the position of the atom i , \mathbf{r}_p is equal to $\sum_{i=1}^N \mathbf{r}_i |\mathbf{u}_i(\omega_p)|^2$ and $\mathbf{u}_i(\omega_p) = \mathbf{e}_i(\omega_p) / \sqrt{\mathbf{M}_i}$ is the atomic displacement of the atom i in mode p . The vibrational correlation length gives a measure of the spatial localization of the vibrational modes by indicating that the amplitude of the atomic vibrations decreases significantly beyond this correlation length.

5. CONCLUSIONS

In this work, we have investigated some aspects of the vibrational dynamics of a model of sodium tetrasilicate glass, constructed by combined classical and Car-Parrinello molecular dynamics simulations. Its vibrational dynamics has been then studied using two different approaches - a first-principles one and a classical valence force fields one. The valence force field serves as a natural reference frame for analysis of the character of the vibrational modes. We have also calculated the polarized Raman spectra within the bond polarization approximation and compared with experimental Raman data.

The VDOS calculated by the two methods have very similar shape, especially for the low-frequency bands below 550 cm^{-1} . In the high-frequency range, the VFF partial VDOS for the Si, BO and NBO atoms are shifted to higher frequencies and they are narrower. As the *ab initio* forces are calculated from first principles, this indicates a need for: (i) an adjustment of the VFF force constants in order to minimize the frequency shifts and (ii) additional analysis of the vibrational modes showing what kind of extra terms must be included in the VFF potential in order to increase the number of low-frequency modes and the localization of the high-frequency modes.

The comparison of the calculated and experimental VV Raman spectra shows that a good agreement between the relative intensities of the low- and high-frequency bands is achieved using the CP eigenmodes. This indicates that the corresponding BPA parameters are approximately correct and can be used for calculation of the VV Raman spectra of structural models of silicate glasses that are still too large to be fully treated *ab initio*. However, despite the fact that the CP eigenvectors are calculated from first principles they do not reproduce well the position of the mid-frequency VV and VH Raman bands at about 780 cm^{-1} . Additional improvement of the BPA parameters describing the high-frequency depolarized Raman bands is also necessary.

The analysis of the character of the vibrational modes shows that the localization of the CP vibrational modes is stronger than of the VFF modes, in particular on the top of the low-frequency band ($\approx 200\text{ cm}^{-1}$) and on both sides of the high-frequency bands.

ACKNOWLEDGMENTS

The financial support from the German Science Foundation under project SFB 408 for N. Zotov is kindly acknowledged. We would like to thank Magali Benoit for very interesting and stimulating discussions. The *ab initio* simulations have been performed on the IBM/SP3 in CINES, Montpellier, FRANCE.

REFERENCES

- [1] E. Courtens, M. Foret, B. hehlen, R. Vacher, Solid State Commun. **117** (2001) 187.
- [2] R. Dupree, D. Holland, P.W. McMillan and R.F. Pettifer, J. Non-Cryst. Sol. **68**, (1984) 399; J. F. Emerson, P.E. Stallworth and P.J. Bray, J. Non-Cryst. Sol. **113**, (1989) 253 ; G. H. Wolf, D.J. Durben and P. F. Mc Millan, J. Chem. Phys. **93**, 2280 (1990); H. Maekawa, T. Maekawa, K. Kawamura and T. Yokokawa, J. Non-Cryst. Sol. **127**, (1991) 53 ; J. Kümmerlen, L. H. Merwin, A. Sebald and H. Keppler, J. Phys. Chem. **96**, (1992) 6405 ; N. Zotov, H. Keppler, A.C. Hannon and A.K. Soper, J. Non-Cryst. Sol. **202**, (1996) 153 .
- [3] N. Zotov and H. Keppler, Phys. Chem. Minerals **26**, (1998) 107.
- [4] A. A. Tesar and A. K. Varshneya, J. Chem. Phys. **87**, (1987) 2986 ; C. Huang and A. N. Cormack, J. Chem. Phys. **93**, (1990) 8180 ; C. Huang and A. N. Cormack, J. Chem. Phys. **95**, (1991) 3634 ; J. Oviedo and F. Sanz, Phys. Rev. B **58**, (1998) 9047 ; E. Sunyer, P. Jund and R. Jullien, Phys. Rev. **65**, (2002) 214203.
- [5] N. Zotov, I. Ebbsjö, D. Timpel and H. Keppler, Phys. Rev. B, **60** (1999) 6383.
- [6] S. Ispas, M. Benoit, P. Jund and R. Jullien, Phys. Rev. B, **64** (2001) 214206.
- [7] S. Ispas, M. Benoit, P. Jund and R. Jullien, J. Non. Cryst. Sol. **307-310** (2002) 946.
- [8] N. P. Bansal and R. H. Doremus, *Handbook of Glass Properties*, Academic Press, INC., New York (1986).
- [9] M. Benoit, S. Ispas, P. Jund and R. Jullien, Euro. Phys. J. B **13**, (2000) 631.
- [10] M. Benoit and W. Kob, Europhys. Lett. **60**, (2002) 269.
- [11] B.W. H. van Best, G.J. Kramer and R.A. van Santen, Phys. Rev. Lett., **64**, (1990) 1955.
- [12] J. Horbach, W. Kob and K. Binder, Chem. Geol. **174**, (2001) 87.
- [13] R. Car and M. Parrinello, Phys. Rev. Lett. **55**, (1985) 2471.
- [14] D. Marx and J. Hutter, in *Modern methods and Algorithms of Quantum Chemistry*, ed. J. Grotendorst, Forschungszentrum Jülich, NIC Series, **1**, (2000) 301.
- [15] CPMD Version 3.3, J. Hutter, A. Alavi, T. Deutsch, M. Bernasconi, S. Goedecker, D. Marx, M. Tuckerman and M. Parrinello, MPI für Festkörperforschung and IBM Research (1995-1999).
- [16] N. Trouiller and J.L Martins, Phys. Rev. B **43**, (1991) 1993.
- [17] B. Michailova, N. Zotov, M. Marinov and L. Konstantinov, J. Non-Cryst. Solids **168**, (1994) 265.
- [18] R. Alben, D. Weaire, J.E. Smith Jr., M.M. Brodsky, Phys. Rev. B **11**, (1975) 2271.
- [19] Umari, A. Pasquarello, A. Dal Corso, Phys. Rev. B **64**, (2001) 094305.
- [20] N. Zotov, J. Phys.: Condens. Matter **14** (2002) 11655.
- [21] R. J. Bell, Methods Comput. Phys. **15** (1976) 215.
- [22] S.N. Taraskin and S.R. Elliott, Phys. Rev. B, **56** (1997) 8605.
- [23] M. Marinov and N. Zotov, Phys. Rev. B, **55** (1997) 2938.

FIGURE CAPTIONS

FIGURE 1 : Vibrational densities of states of the *ab initio* NS4 glass model obtained within a first principles approach (solid line) and within a classical valence-force-field approximation (dashed line).

FIGURE 2 : Frequency dependence of the VV (a) and the VH (b) Raman intensities calculated within the bond-polarizability approximation using the *ab initio* eigen modes (dotted lines) and the classical VFF eigenmodes (dashed lines). The solid lines are the experimental spectra.

FIGURE 3 : Partial VDOS for Si (a), BO (b), NBO (c) and Na (d) atoms calculated using the two sets of eigenfrequencies and normal modes. The solid lines are the CP partial VDOS, while the dashed lines are the VFF partial VDOS.

FIGURE 4 : a) and b) Frequency dependence of the p_c and of the L_c in the CP case; c) and d) Frequency dependence of the p_c and of the L_c in the VFF case. The horizontal lines at a height equal to 5.405 Å (i.e. half of our simulation box length) are drawn as a guide for the eye in order to estimate the number of the normal modes with correlation length smaller or bigger than this value.

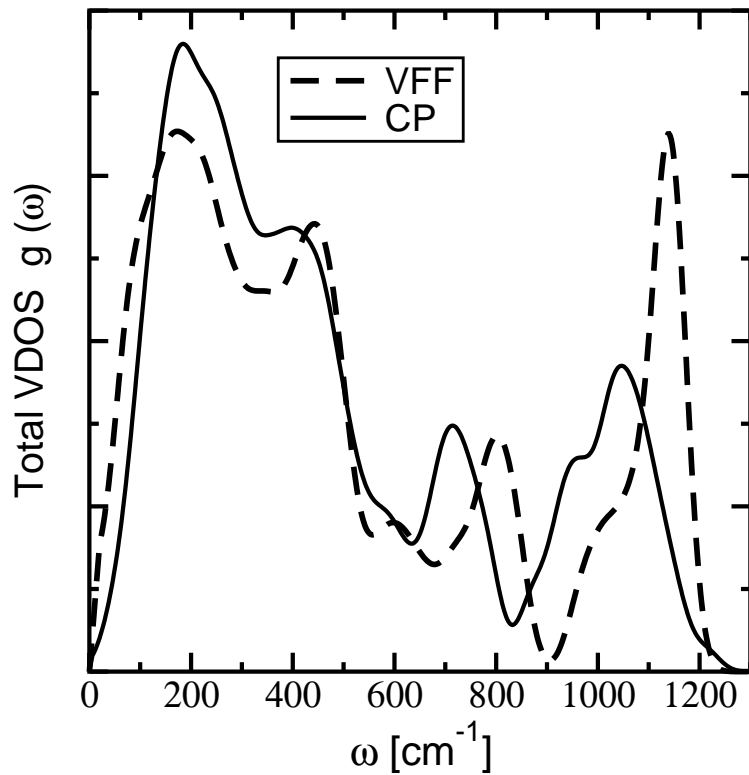


FIG. 1.

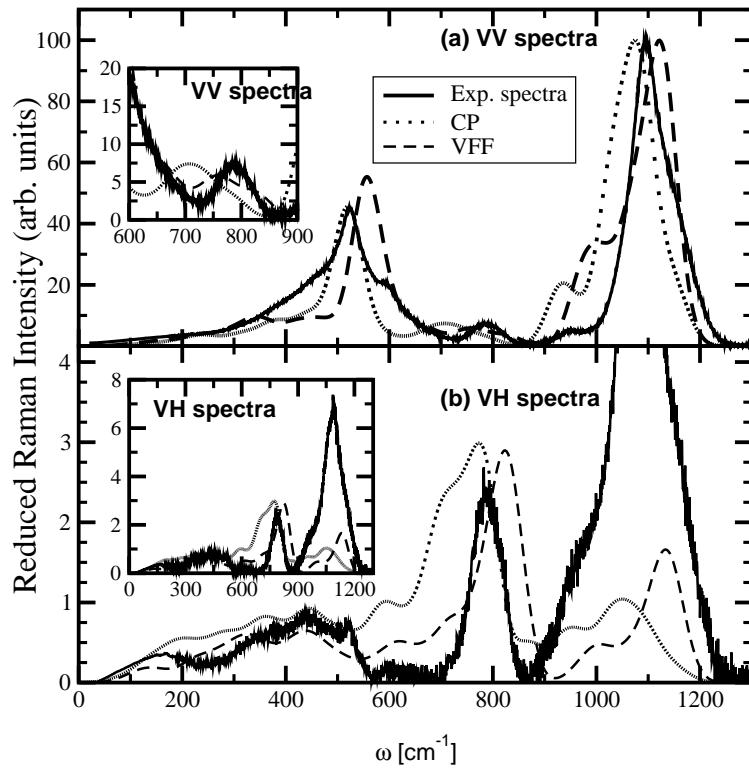


FIG. 2.

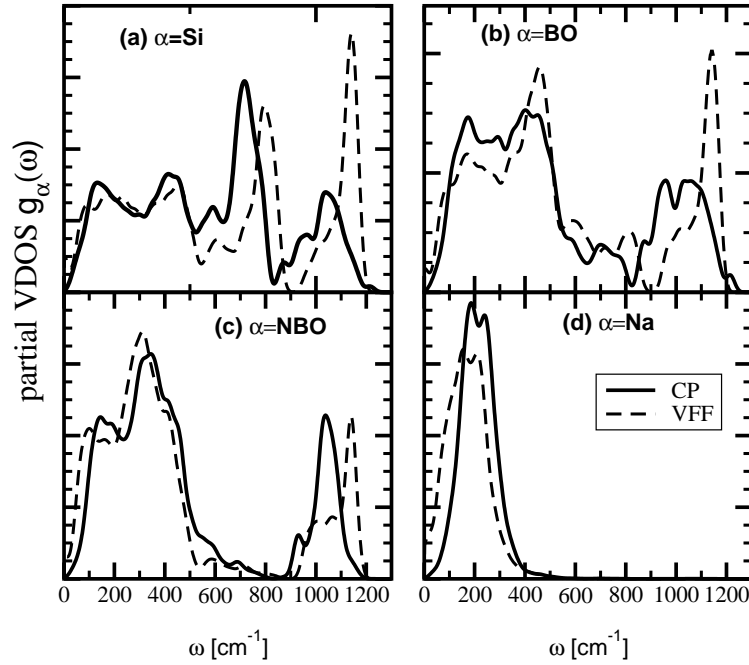


FIG. 3.

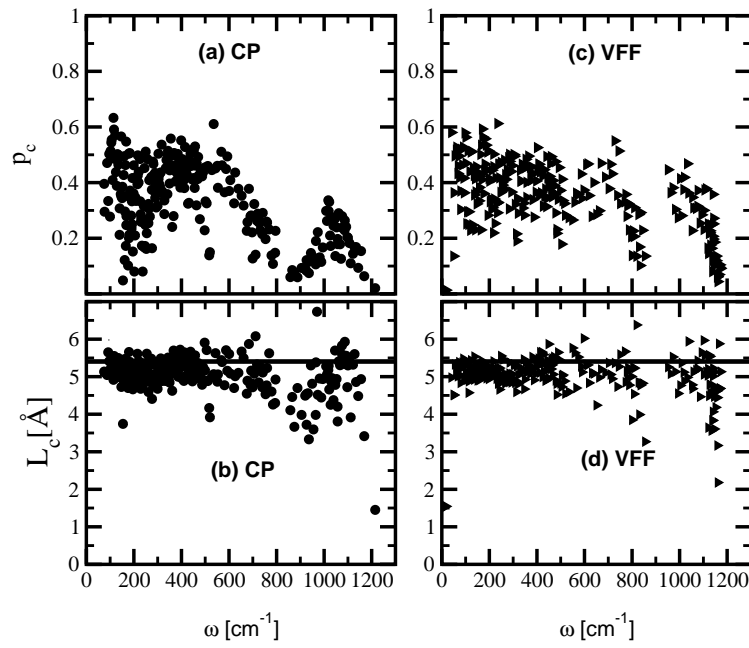


FIG. 4.